
Data-Efficient Realized Volatility Forecasting with Vision Transformers

Anonymous Author(s)

Affiliation

Address

email

Abstract

1 Recent work in financial machine learning has shown the virtue of complexity:
2 the phenomenon by which deep learning methods capable of learning highly
3 nonlinear relationships outperform simpler approaches in financial forecasting.
4 While transformer architectures like Informer have shown promise for financial time
5 series forecasting, the application of transformer models for options data remains
6 largely unexplored. We conduct preliminary studies towards the development of
7 a transformer model for options data by training the Vision Transformer (ViT)
8 architecture, typically used in modern image recognition and classification systems,
9 to predict the realized volatility of an asset over the next 30 days from its implied
10 volatility surface (augmented with date information) for a single day. We show
11 that the ViT can learn seasonal patterns and nonlinear features from the IV surface,
12 suggesting a promising direction for model development.

13 1 Background

14 The implied volatility surface (IV surface) of an optionable asset encodes information about market
15 dynamics and sentiment, the future realized volatility of the asset, and the probability distribution of
16 its return Bali et al. [2022]. Traders construct features from the IV surface to infer this information
17 using options pricing theory or empirical observations. Recent work in financial machine learning has
18 also discovered the virtue of complexity: Gu et al. [2020], Didisheim et al. [2023] the existence of
19 highly nonlinear features in financial data which can be extracted using neural networks, contradicting
20 prior assumptions that financial returns can be explained by a small number of predictive factors.
21 However, machine learning methods are difficult to apply to financial data because the data itself
22 is noisy and limited in scale. For example, our entire preprocessed dataset totals 6.1 GB while text
23 corpora used to train frontier LLMs contain multiple terabytes of data Liu et al. [2024].

24 2 Prior Work

25 The use of neural networks to identify nonlinear patterns in financial data is investigated extensively
26 in Gu et al. [2020]. Other examples include overparametrized factor models with more factors than
27 assets under observation Didisheim et al. [2023], Transformer-based time series forecasting Zhou
28 et al. [2021], and structured approaches to machine learning in finance Dixon and Halperin [2019].
29 Neural networks have also been applied to generate smooth, arbitrage-free IV surfaces from raw
30 option prices Ackerer et al. [2020], Wiedemann et al. [2025]. However, fewer researchers have
31 investigated deep learning for predictions from IV surfaces. Previous approaches include the use of
32 hand-constructed features Neuhierl et al. [2022] or convolutional neural networks (CNNs) Kelly et al.
33 [2023], with the latter using the IV surface on the last trading day of the month to predict the monthly
34 return of the next month. We train Vision Transformer (ViT) models on IV surfaces, treating them

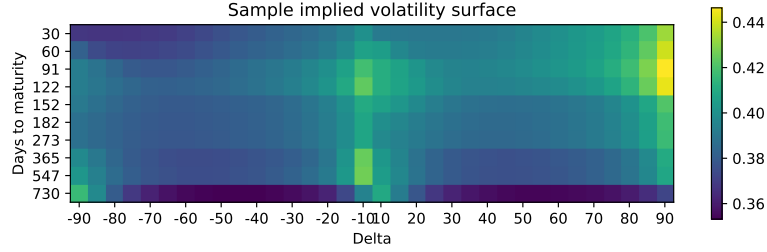


Figure 1: IV surface for NVDA stock on 2021-04-13, presented as a one-channel image instead of the traditional three-dimensional surface. Negative deltas correspond to puts.

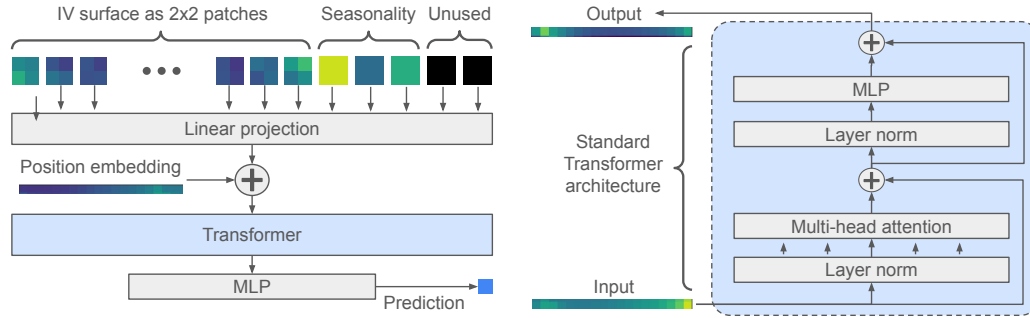


Figure 2: Vision transformer architecture (left) on our data, with more detailed schematic of the standard transformer architecture used in our model (right). In the deep Vision Transformer, the MLP layer in the Transformer model is repeated.

35 as small, single-channel images. ViTs on images require less computational cost than CNNs and
 36 provide more stable training performance Dosovitskiy et al. [2021]; thus we hypothesize they will be
 37 more robust to noisy data and outliers.

38 3 Methodology

39 3.1 Data preparation

40 We use the OptionMetrics IvyDB implied volatility, a grid of smoothed interpolated values with
 41 implied δ of the option on one axis and number of days to maturity on the other; and realized volatility
 42 calculated by OptionMetrics over $n = 28$ calendar days, using the standard deviation on the daily log
 43 return. Following Kelly et al. [2023], we split data by year and month and drop any samples with
 44 incomplete data, producing a full dataset of 4,259,070 rows between 2012 and 2022. We augment the
 45 IV surface with the month, day, and day of the week of the observation, scaled to values in $[0, 1]$, to
 46 allow the model to capture seasonal trends (Figure 1). See Appendix A for details.

47 3.2 Model Architecture

48 We tested both deep and wide ViT architectures, adapting the original ViT model Dosovitskiy et al.
 49 [2021] for single-channel matrices of size 10×36 instead of traditional images¹. Because the ViT
 50 outputs a vector, we add a small four-layer MLP to produce the final real-valued prediction. We
 51 study the performance of this model on our dataset, varying the number of layers and the number of
 52 parameters per layer. Model scaling is of particular interest, as we show that small models can be
 53 trained on limited data and achieve strong performance in the task of forecasting realized volatility.
 54 We compare our model against a baseline multilayer perceptron (MLP) on the flattened IV surface,
 55 observing that the ViT architecture outperforms the MLP. The MLP is also more difficult to train,
 56 requiring early stopping, batch normalization, and multiple training attempts with the best model
 57 selected at the end.

¹Model definitions and code to reproduce all results will be released with the final version of this paper.

Model	ViT_0.005M_wide	ViT_0.12M_deep	ViT_0.17M_wide
# Params	46466	122114	170754
Model	ViT_0.5M_deep	ViT_0.5M_wide	ViT_1.7M
# Params	469506	545282	1732610

Table 1: Model definitions with number of parameters; full definitions are in Appendix B.

3.3 Training

We define train and test sets such that if the test year is y_i , the corresponding n training years are $y_{i-n}, y_{i-n+1}, \dots, y_{i-1}$. We pay close attention to the choice of optimizer, learning rate schedule, and loss function to achieve more stable and efficient training. Prior work has applied early stopping, regularization, and ensembling to overcome the challenges of training on financial data Gu et al. [2020]. We apply batch normalization, a form of regularization, and Xavier initialization Glorot and Bengio [2010] in the MLP prediction component of our model. Our training procedure follows the process used to train text foundation models such as DeepSeek-v3 DeepSeek-AI et al. [2025] and Llama Grattafiori et al. [2024], scaled down for the available data. We use a cosine annealing learning rate scheduler², introduced in Loshchilov and Hutter [2017] and shown to achieve strong performance on ImageNet Goyal et al. [2018] with large batch sizes. (We use a batch size of 2048 for all experiments.) We use the AdamW optimizer Loshchilov and Hutter [2019] and select the best-performing model from all training epochs. To reduce the impact of outliers, we use the Huber loss l , a convex loss function that is quadratic for small values of $\hat{y} - y$ and linear for large values. We report the model’s R^2 on unseen test data.

$$\ell_{\text{huber}}(\hat{y}, y) = \begin{cases} \frac{1}{2} (\hat{y} - y)^2 & |\hat{y} - y| \leq d \\ d \cdot (|\hat{y} - y| - \frac{1}{2}d) & \text{otherwise} \end{cases} \quad (1)$$

We evaluate both deep and wide ViT models of varying sizes. The deep models have four MLP layers in the Transformer module (see Figure 2), while the wide models have one MLP layer in this module.

4 Results

We study the performance of the models listed in Table 1 to predict the realized volatility of an asset over the next 30 days when trained on varying dataset sizes. Because one of the challenges for financial machine learning is the availability of data, we evaluate model performance when trained on one, four, or ten years of data, finding that smaller models (.05-.17M) can perform well when trained on smaller datasets but collapse on large ones,

while the 0.5M models do not improve on the smaller models. The 1.7M model yields the best performance but requires the full ten years of training data (Figure 3). Additionally, all models perform poorly if the training and test data are dissimilar (Figure 4). In this case, the small models provide an advantage as they could be retrained as new data becomes available. Model performance varies across different market conditions, with all models showing reduced performance when tested on 2020 data (Figure 4). The best model is ViT_1.7M trained on 2012-2021 data, which achieves $R^2 = 0.41$ on the 2022 test set (Figure 3). All ViT models reach their maximum R^2 within one or two epochs, with further training causing overfitting (Appendix C).

Key findings: ViT models can extract nonlinear features from IV surfaces, with small models requiring as little as one year of data to train. Despite the limited availability of market data, **designing model architectures and training processes to fit the available data can enable the development of transformer models for financial forecasting tasks.**

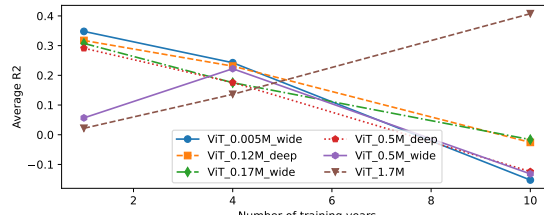


Figure 3: Effect of dataset size on model R^2 . Where multiple train-test splits are possible, average R^2 is reported.

²<https://github.com/katsura-jp/pytorch-cosine-annealing-with-warmup>, called with parameters `scheduler.scheduler_first_cycle_steps = 200`, `scheduler.scheduler_max_lr = 0.01`, `scheduler.scheduler_min_lr = 0.001`, `scheduler.scheduler_warmup_steps = 100`, `scheduler.scheduler_gamma = 0.95`.

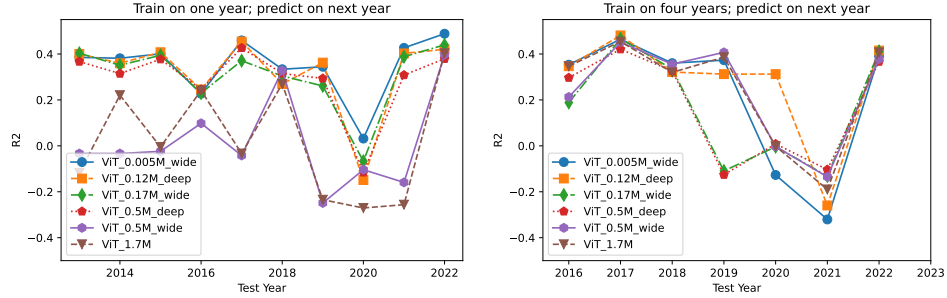


Figure 4: Training on one year (left) or four (right) and predicting the 30-day realized volatility on the next year, for data between 2012-2022. The performance drop for the test year 2020 reflects market disruption during the COVID pandemic. In practice one could iteratively retrain the models; note that the small models recover their performance on the 2021 test sample.

100 5 Ablation Testing

101 We test our ViT model against two ablations: the ViT model on the IV surface with no seasonality
 102 augmentation, and an MLP-only model with roughly the same number of parameters. Full definitions
 103 of these models are provided in Appendix B. Removing the seasonality information has a small nega-
 104 tive effect, suggesting the model is primarily extracting nonlinear patterns from the IV surface. The
 105 MLP-only models do not perform well, with larger model sizes actually yielding worse performance.

Model	# Train Years	Baseline R^2	No seasonality
ViT_0.5M_deep	4	0.35	0.35
ViT_0.5M_wide	4	0.37	0.35
ViT_1.7M	10	0.41	0.38

Table 2: Effect of removing seasonality information.

Model	ViT Params	Baseline R^2	MLP Model	MLP Only R^2	MLP Params
ViT_0.12M_deep	122114	0.27	MLP_0_12	0.29	114842
ViT_0.17M_wide	170754	0.37	MLP_0_17	0.29	174722
ViT_0.5M_deep	469506	0.35	MLP_0_5	0.17	515252
ViT_0.5M_wide	545282	0.37	MLP_0_5	0.17	515252

Table 3: Comparison between ViT and MLP-only architectures with similar parameter counts. All models were trained on 4 years of data from 2018-2021 and tested on 2022.

106

107 6 Planned and Future Work

108 This is an ongoing project with many interesting directions. Our top priority is to study the potential
 109 for transfer learning on IV surfaces: the ability to fine-tune a model or retrain only the final stages
 110 of the model, such as regressor or classifier layers, to predict a different target value. ViT models
 111 trained on image datasets exhibit this property and are often fine-tuned for specific classification tasks
 112 in medical or scientific imaging Li et al. [2021]. We are also interested in investigating whether the
 113 ViT model can learn output vectors that generalize to other prediction tasks if the MLP predictor is
 114 retrained. We tested for this capability using the task of predicting the asset’s return over the next 28
 115 days and did not observe it; however this task is more difficult than predicting the realized volatility.
 116 Following our theme of applying foundation model techniques to financial data, we could compare
 117 ensembling, applied in Kelly et al. [2023], against a Mixture-of-Experts architecture DeepSeek-AI
 118 et al. [2025]. Finally, as there is clearly a link between model size, dataset size and performance,
 119 a theoretical understanding of the information content of IV surfaces could provide guidance for
 120 optimal data sampling to improve model performance.

121 **References**

- 122 Damien Ackerer, Natasa Tagasovska, and Thibault Vatter. Deep smoothing of the implied volatility
123 surface, 2020. URL <https://arxiv.org/abs/1906.05065>.
- 124 Turan G Bali, Fousseni Chabi-Yo, and Scott Murray. A factor model for stock returns based on option
125 prices. *Available at SSRN 3487947*, 2022.
- 126 DeepSeek-AI, Aixin Liu, Bei Feng, Bing Xue, Bingxuan Wang, Bochao Wu, Chengda Lu, Chenggang
127 Zhao, Chengqi Deng, Chenyu Zhang, Chong Ruan, Damai Dai, Daya Guo, Dejian Yang, Deli
128 Chen, Dongjie Ji, Erhang Li, Fangyun Lin, Fucong Dai, Fuli Luo, Guangbo Hao, Guanting Chen,
129 Guowei Li, H. Zhang, Han Bao, Hanwei Xu, Haocheng Wang, Haowei Zhang, Honghui Ding,
130 Huajian Xin, Huazuo Gao, Hui Li, Hui Qu, J. L. Cai, Jian Liang, Jianzhong Guo, Jiaqi Ni, Jiashi
131 Li, Jiawei Wang, Jin Chen, Jingchang Chen, Jingyang Yuan, Junjie Qiu, Junlong Li, Junxiao Song,
132 Kai Dong, Kai Hu, Kaige Gao, Kang Guan, Kexin Huang, Kuai Yu, Lean Wang, Lecong Zhang,
133 Lei Xu, Leyi Xia, Liang Zhao, Litong Wang, Liyue Zhang, Meng Li, Miaoqun Wang, Mingchuan
134 Zhang, Minghua Zhang, Minghui Tang, Mingming Li, Ning Tian, Panpan Huang, Peiyi Wang,
135 Peng Zhang, Qiancheng Wang, Qihao Zhu, Qinyu Chen, Qiushi Du, R. J. Chen, R. L. Jin, Ruiqi
136 Ge, Ruisong Zhang, Ruizhe Pan, Runji Wang, Runxin Xu, Ruoyu Zhang, Ruyi Chen, S. S. Li,
137 Shanghao Lu, Shangyan Zhou, Shanhuang Chen, Shaoqing Wu, Shengfeng Ye, Shengfeng Ye,
138 Shirong Ma, Shiyu Wang, Shuang Zhou, Shuiping Yu, Shunfeng Zhou, Shuting Pan, T. Wang,
139 Tao Yun, Tian Pei, Tianyu Sun, W. L. Xiao, Wangding Zeng, Wanbiao Zhao, Wei An, Wen Liu,
140 Wenfeng Liang, Wenjun Gao, Wenqin Yu, Wentao Zhang, X. Q. Li, Xiangyue Jin, Xianzu Wang,
141 Xiao Bi, Xiaodong Liu, Xiaohan Wang, Xiaojin Shen, Xiaokang Chen, Xiaokang Zhang, Xiaosha
142 Chen, Xiaotao Nie, Xiaowen Sun, Xiaoxiang Wang, Xin Cheng, Xin Liu, Xin Xie, Xingchao Liu,
143 Xingkai Yu, Xinnan Song, Xinxia Shan, Xinyi Zhou, Xinyu Yang, Xinyuan Li, Xuecheng Su,
144 Xuheng Lin, Y. K. Li, Y. Q. Wang, Y. X. Wei, Y. X. Zhu, Yang Zhang, Yanhong Xu, Yanhong
145 Xu, Yanping Huang, Yao Li, Yao Zhao, Yaofeng Sun, Yaohui Li, Yaohui Wang, Yi Yu, Yi Zheng,
146 Yichao Zhang, Yifan Shi, Yiliang Xiong, Ying He, Ying Tang, Yishi Piao, Yisong Wang, Yixuan
147 Tan, Yiyang Ma, Yiyuan Liu, Yongqiang Guo, Yu Wu, Yuan Ou, Yuchen Zhu, Yuduan Wang, Yue
148 Gong, Yuheng Zou, Yujia He, Yukun Zha, Yunfan Xiong, Yunxian Ma, Yuting Yan, Yuxiang Luo,
149 Yuxiang You, Yuxuan Liu, Yuyang Zhou, Z. F. Wu, Z. Z. Ren, Zehui Ren, Zhangli Sha, Zhe Fu,
150 Zhean Xu, Zhen Huang, Zhen Zhang, Zhenda Xie, Zhengyan Zhang, Zhewen Hao, Zhibin Guo,
151 Zhicheng Ma, Zhigang Yan, Zhihong Shao, Zhipeng Xu, Zhiyu Wu, Zhongyu Zhang, Zhuoshu
152 Li, Zihui Gu, Zijia Zhu, Zijun Liu, Zilin Li, Ziwei Xie, Ziyang Song, Ziyi Gao, and Zizheng Pan.
153 Deepseek-v3 technical report, 2025. URL <https://arxiv.org/abs/2412.19437>.
- 154 Antoine Didisheim, Shikun (Barry) Ke, Bryan T. Kelly, and Semyon Malamud. Complexity in factor
155 pricing models. NBER Working Papers 31689, National Bureau of Economic Research, Inc, Sep
156 2023. URL <https://ideas.repec.org/p/nbr/nberwo/31689.html>.
- 157 Matthew Dixon and Igor Halperin. The four horsemen of machine learning in finance. *SSRN*
158 *Electronic Journal*, 01 2019. doi: 10.2139/ssrn.3453564.
- 159 Alexey Dosovitskiy, Lucas Beyer, Alexander Kolesnikov, Dirk Weissenborn, Xiaohua Zhai, Thomas
160 Unterthiner, Mostafa Dehghani, Matthias Minderer, Georg Heigold, Sylvain Gelly, Jakob Uszkoreit,
161 and Neil Houlsby. An image is worth 16x16 words: Transformers for image recognition at scale,
162 2021. URL <https://arxiv.org/abs/2010.11929>.
- 163 Xavier Glorot and Yoshua Bengio. Understanding the difficulty of training deep feedforward neural
164 networks. In *Proceedings of the thirteenth international conference on artificial intelligence and*
165 *statistics*, pages 249–256. JMLR Workshop and Conference Proceedings, 2010.
- 166 Priya Goyal, Piotr Dollár, Ross Girshick, Pieter Noordhuis, Lukasz Wesolowski, Aapo Kyrola,
167 Andrew Tulloch, Yangqing Jia, and Kaiming He. Accurate, large minibatch sgd: Training imagenet
168 in 1 hour, 2018. URL <https://arxiv.org/abs/1706.02677>.
- 169 Aaron Grattafiori, Abhimanyu Dubey, Abhinav Jauhri, Abhinav Pandey, Abhishek Kadian, Ahmad
170 Al-Dahle, Aiesha Letman, Akhil Mathur, Alan Schelten, Alex Vaughan, Amy Yang, Angela Fan,
171 Anirudh Goyal, Anthony Hartshorn, Aobo Yang, Archi Mitra, Archie Sravankumar, Artem Korenev,
172 Arthur Hinsvark, Arun Rao, Aston Zhang, Aurelien Rodriguez, Austen Gregerson, Ava Spataru,
173 Baptiste Roziere, Bethany Biron, Binh Tang, Bobbie Chern, Charlotte Caucheteux, Chaya Nayak,

174 Chloe Bi, Chris Marra, Chris McConnell, Christian Keller, Christophe Touret, Chunyang Wu,
 175 Corinne Wong, Cristian Canton Ferrer, Cyrus Nikolaidis, Damien Allonsius, Daniel Song, Danielle
 176 Pintz, Danny Livshits, Danny Wyatt, David Esiobu, Dhruv Choudhary, Dhruv Mahajan, Diego
 177 Garcia-Olano, Diego Perino, Dieuwke Hupkes, Egor Lakomkin, Ehab AlBadawy, Elina Lobanova,
 178 Emily Dinan, Eric Michael Smith, Filip Radenovic, Francisco Guzmán, Frank Zhang, Gabriel
 179 Synnaeve, Gabrielle Lee, Georgia Lewis Anderson, Govind Thattai, Graeme Nail, Gregoire Mialon,
 180 Guan Pang, Guillem Cucurell, Hailey Nguyen, Hannah Korevaar, Hu Xu, Hugo Touvron, Iliyan
 181 Zarov, Imanol Arrieta Ibarra, Isabel Kloumann, Ishan Misra, Ivan Evtimov, Jack Zhang, Jade Copet,
 182 Jaewon Lee, Jan Geffert, Jana Vranes, Jason Park, Jay Mahadeokar, Jeet Shah, Jelmer van der Linde,
 183 Jennifer Billock, Jenny Hong, Jenya Lee, Jeremy Fu, Jianfeng Chi, Jianyu Huang, Jiawen Liu, Jie
 184 Wang, Jiecao Yu, Joanna Bitton, Joe Spisak, Jongsoo Park, Joseph Rocca, Joshua Johnstun, Joshua
 185 Saxe, Junteng Jia, Kalyan Vasuden Alwala, Karthik Prasad, Kartikeya Upasani, Kate Plawiak,
 186 Ke Li, Kenneth Heafield, Kevin Stone, Khalid El-Arini, Krithika Iyer, Kshitiz Malik, Kuenley
 187 Chiu, Kunal Bhalla, Kushal Lakhotia, Lauren Rantala-Yearly, Laurens van der Maaten, Lawrence
 188 Chen, Liang Tan, Liz Jenkins, Louis Martin, Lovish Madaan, Lubo Malo, Lukas Blecher, Lukas
 189 Landzaat, Luke de Oliveira, Madeline Muzzi, Mahesh Pasupuleti, Mannat Singh, Manohar Paluri,
 190 Marcin Kardas, Maria Tsimpoukelli, Mathew Oldham, Mathieu Rita, Maya Pavlova, Melanie
 191 Kambadur, Mike Lewis, Min Si, Mitesh Kumar Singh, Mona Hassan, Naman Goyal, Narjes
 192 Torabi, Nikolay Bashlykov, Nikolay Bogoychev, Niladri Chatterji, Ning Zhang, Olivier Duchenne,
 193 Onur Çelebi, Patrick Alrassy, Pengchuan Zhang, Pengwei Li, Petar Vasic, Peter Weng, Prajwal
 194 Bhargava, Pratik Dubal, Praveen Krishnan, Punit Singh Koura, Puxin Xu, Qing He, Qingxiao Dong,
 195 Ragavan Srinivasan, Raj Ganapathy, Ramon Calderer, Ricardo Silveira Cabral, Robert Stojnic,
 196 Roberta Raileanu, Rohan Maheswari, Rohit Girdhar, Rohit Patel, Romain Sauvestre, Ronnie
 197 Polidoro, Roshan Sumbaly, Ross Taylor, Ruan Silva, Rui Hou, Rui Wang, Saghar Hosseini, Sahana
 198 Chennabasappa, Sanjay Singh, Sean Bell, Seohyun Sonia Kim, Sergey Edunov, Shaoliang Nie,
 199 Sharan Narang, Sharath Rapparthi, Sheng Shen, Shengye Wan, Shruti Bhosale, Shun Zhang, Simon
 200 Vandenhende, Soumya Batra, Spencer Whitman, Sten Sootla, Stephane Collot, Suchin Gururangan,
 201 Sydney Borodinsky, Tamar Herman, Tara Fowler, Tarek Sheasha, Thomas Georgiou, Thomas
 202 Scialom, Tobias Speckbacher, Todor Mihaylov, Tong Xiao, Ujjwal Karn, Vedanuj Goswami,
 203 Vibhor Gupta, Vignesh Ramanathan, Viktor Kerkez, Vincent Gonguet, Virginie Do, Vish Vogeti,
 204 Vitor Albiero, Vladan Petrovic, Weiwei Chu, Wenhan Xiong, Wenyin Fu, Whitney Meers, Xavier
 205 Martinet, Xiaodong Wang, Xiaofang Wang, Xiaoqing Ellen Tan, Xide Xia, Xinfeng Xie, Xuchao
 206 Jia, Xuwei Wang, Yaelle Goldschlag, Yashesh Gaur, Yasmine Babaei, Yi Wen, Yiwen Song,
 207 Yuchen Zhang, Yue Li, Yuning Mao, Zacharie Delpierre Coudert, Zheng Yan, Zhengxing Chen, Zoe
 208 Papakipos, Aaditya Singh, Aayushi Srivastava, Abha Jain, Adam Kelsey, Adam Shajnfeld, Adithya
 209 Gangidi, Adolfo Victoria, Ahuva Goldstand, Ajay Menon, Ajay Sharma, Alex Boesenberg, Alexei
 210 Baevski, Allie Feinstein, Amanda Kallet, Amit Sangani, Amos Teo, Anam Yunus, Andrei Lupu,
 211 Andres Alvarado, Andrew Caples, Andrew Gu, Andrew Ho, Andrew Poulton, Andrew Ryan, Ankit
 212 Ramchandani, Annie Dong, Annie Franco, Anuj Goyal, Aparajita Saraf, Arkabandhu Chowdhury,
 213 Ashley Gabriel, Ashwin Barambe, Assaf Eisenman, Azadeh Yazdan, Beau James, Ben Maurer,
 214 Benjamin Leonhardi, Bernie Huang, Beth Loyd, Beto De Paola, Bhargavi Paranjape, Bing Liu,
 215 Bo Wu, Boyu Ni, Braden Hancock, Bram Wasti, Brandon Spence, Brani Stojkovic, Brian Gamido,
 216 Britt Montalvo, Carl Parker, Carly Burton, Catalina Mejia, Ce Liu, Changhan Wang, Changkyu
 217 Kim, Chao Zhou, Chester Hu, Ching-Hsiang Chu, Chris Cai, Chris Tindal, Christoph Feichtenhofer,
 218 Cynthia Gao, Damon Civin, Dana Beaty, Daniel Kreymer, Daniel Li, David Adkins, David Xu,
 219 Davide Testuggine, Delia David, Devi Parikh, Diana Liskovich, Didem Foss, Dingkang Wang, Duc
 220 Le, Dustin Holland, Edward Dowling, Eissa Jamil, Elaine Montgomery, Eleonora Presani, Emily
 221 Hahn, Emily Wood, Eric-Tuan Le, Erik Brinkman, Esteban Arcaute, Evan Dunbar, Evan Smothers,
 222 Fei Sun, Felix Kreuk, Feng Tian, Filippos Kokkinos, Firat Ozgenel, Francesco Caggioni, Frank
 223 Kanayet, Frank Seide, Gabriela Medina Florez, Gabriella Schwarz, Gada Badeer, Georgia Swee,
 224 Gil Halpern, Grant Herman, Grigory Sizov, Guangyi, Zhang, Guna Lakshminarayanan, Hakan Inan,
 225 Hamid Shojanazeri, Han Zou, Hannah Wang, Hanwen Zha, Haroun Habeeb, Harrison Rudolph,
 226 Helen Suk, Henry Aspegren, Hunter Goldman, Hongyuan Zhan, Ibrahim Damlaj, Igor Molybog,
 227 Igor Tufanov, Ilias Leontiadis, Irina-Elena Veliche, Itai Gat, Jake Weissman, James Geboski, James
 228 Kohli, Janice Lam, Japhet Asher, Jean-Baptiste Gaya, Jeff Marcus, Jeff Tang, Jennifer Chan, Jenny
 229 Zhen, Jeremy Reizenstein, Jeremy Teboul, Jessica Zhong, Jian Jin, Jingyi Yang, Joe Cummings,
 230 Jon Carvill, Jon Shepard, Jonathan McPhie, Jonathan Torres, Josh Ginsburg, Junjie Wang, Kai
 231 Wu, Kam Hou U, Karan Saxena, Kartikay Khandelwal, Katayoun Zand, Kathy Matosich, Kaushik
 232 Veeraraghavan, Kelly Michelena, Keqian Li, Kiran Jagadeesh, Kun Huang, Kunal Chawla, Kyle

233 Huang, Lailin Chen, Lakshya Garg, Lavender A, Leandro Silva, Lee Bell, Lei Zhang, Liangpeng
234 Guo, Licheng Yu, Liron Moshkovich, Luca Wehrstedt, Madian Khabza, Manav Avalani, Manish
235 Bhatt, Martynas Mankus, Matan Hasson, Matthew Lennie, Matthias Reso, Maxim Groshev, Maxim
236 Naumov, Maya Lathi, Meghan Keneally, Miao Liu, Michael L. Seltzer, Michal Valko, Michelle
237 Restrepo, Mihir Patel, Mik Vyatskov, Mikayel Samvelyan, Mike Clark, Mike Macey, Mike Wang,
238 Miquel Jubert Hermoso, Mo Metanat, Mohammad Rastegari, Munish Bansal, Nandhini Santhanam,
239 Natascha Parks, Natasha White, Navyata Bawa, Nayan Singhal, Nick Egebo, Nicolas Usunier,
240 Nikhil Mehta, Nikolay Pavlovich Laptev, Ning Dong, Norman Cheng, Oleg Chernoguz, Olivia
241 Hart, Omkar Salpekar, Ozlem Kalinli, Parkin Kent, Parth Parekh, Paul Saab, Pavan Balaji, Pedro
242 Rittner, Philip Bontrager, Pierre Roux, Piotr Dollar, Polina Zvyagina, Prashant Ratanchandani,
243 Pritish Yuvraj, Qian Liang, Rachad Alao, Rachel Rodriguez, Rafi Ayub, Raghotham Murthy,
244 Raghu Nayani, Rahul Mitra, Rangaprabhu Parthasarathy, Raymond Li, Rebekkah Hogan, Robin
245 Battey, Rocky Wang, Russ Howes, Ruty Rinott, Sachin Mehta, Sachin Siby, Sai Jayesh Bondu,
246 Samyak Datta, Sara Chugh, Sara Hunt, Sargun Dhillon, Sasha Sidorov, Satadru Pan, Saurabh
247 Mahajan, Saurabh Verma, Seiji Yamamoto, Sharadh Ramaswamy, Shaun Lindsay, Shaun Lindsay,
248 Sheng Feng, Shenghao Lin, Shengxin Cindy Zha, Shishir Patil, Shiva Shankar, Shuqiang Zhang,
249 Shuqiang Zhang, Sinong Wang, Sneha Agarwal, Soji Sajuyigbe, Soumith Chintala, Stephanie
250 Max, Stephen Chen, Steve Kehoe, Steve Satterfield, Sudarshan Govindaprasad, Sumit Gupta,
251 Summer Deng, Sungmin Cho, Sunny Virk, Suraj Subramanian, Sy Choudhury, Sydney Goldman,
252 Tal Remez, Tamar Glaser, Tamara Best, Thilo Koehler, Thomas Robinson, Tianhe Li, Tianjun
253 Zhang, Tim Matthews, Timothy Chou, Tzook Shaked, Varun Vontimitta, Victoria Ajayi, Victoria
254 Montanez, Vijai Mohan, Vinay Satish Kumar, Vishal Mangla, Vlad Ionescu, Vlad Poenaru,
255 Vlad Tiberiu Mihailescu, Vladimir Ivanov, Wei Li, Wenchen Wang, Wenwen Jiang, Wes Bouaziz,
256 Will Constable, Xiaocheng Tang, Xiaojian Wu, Xiaolan Wang, Xilun Wu, Xinbo Gao, Yaniv
257 Kleinman, Yanjun Chen, Ye Hu, Ye Jia, Ye Qi, Yenda Li, Yilin Zhang, Ying Zhang, Yossi Adi,
258 Youngjin Nam, Yu, Wang, Yu Zhao, Yuchen Hao, Yundi Qian, Yunlu Li, Yuzi He, Zach Rait,
259 Zachary DeVito, Zef Rosnbrick, Zhaoduo Wen, Zhenyu Yang, Zhiwei Zhao, and Zhiyu Ma. The
260 llama 3 herd of models, 2024. URL <https://arxiv.org/abs/2407.21783>.

261 Shihao Gu, Bryan Kelly, and Dacheng Xiu. Empirical asset pricing via machine learning. *The Review*
262 *of Financial Studies*, 33(5):2223–2273, 02 2020. ISSN 0893-9454. doi: 10.1093/rfs/hhaa009.
263 URL <https://doi.org/10.1093/rfs/hhaa009>.

264 Bryan T. Kelly, Boris Kuznetsov, Semyon Malamud, and Teng Andrea Xu. Deep learning from
265 implied volatility surfaces. Swiss Finance Institute Research Paper Series 23-60, Swiss Finance
266 Institute, Aug 2023. URL <https://ideas.repec.org/p/chf/rpseri/rp2360.html>.

267 Yanghao Li, Saining Xie, Xinlei Chen, Piotr Dollár, Kaiming He, and Ross B. Girshick. Bench-
268 marking detection transfer learning with vision transformers. *CoRR*, abs/2111.11429, 2021. URL
269 <https://arxiv.org/abs/2111.11429>.

270 Yang Liu, Jiahuan Cao, Chongyu Liu, Kai Ding, and Lianwen Jin. Datasets for large language
271 models: A comprehensive survey, 2024. URL <https://arxiv.org/abs/2402.18041>.

272 Ilya Loshchilov and Frank Hutter. Sgdr: Stochastic gradient descent with warm restarts, 2017. URL
273 <https://arxiv.org/abs/1608.03983>.

274 Ilya Loshchilov and Frank Hutter. Decoupled weight decay regularization, 2019. URL <https://arxiv.org/abs/1711.05101>.

276 Andreas Neuhierl, Xiaoxiao Tang, Rasmus Tangsgaard Varneskov, and Guofu Zhou. Option char-
277 acteristics as cross-sectional predictors. LawFin Working Paper 37, Frankfurt a. M., 2022. URL
278 <https://hdl.handle.net/10419/261467>. urn:nbn:de:hebis:30:3-652441.

279 Ruben Wiedemann, Antoine Jacquier, and Lukas Gonon. Operator deep smoothing for implied
280 volatility, 2025. URL <https://arxiv.org/abs/2406.11520>.

281 Haoyi Zhou, Shanghang Zhang, Jieqi Peng, Shuai Zhang, Jianxin Li, Hui Xiong, and Wancai Zhang.
282 Informer: Beyond efficient transformer for long sequence time-series forecasting, 2021. URL
283 <https://arxiv.org/abs/2012.07436>.

284 **A Data Preparation**

285 **A.1 Identification of Valid Assets**

286 While the IV surfaces and realized volatilities are present in the OptionMetrics IvyDB dataset, we are
287 also interested in predicting the future returns of an asset, which can be calculated using the daily
288 returns in the CRSP (Center for Research in Security Prices) dataset. However, OptionMetrics uses
289 the primary key `secid` and CRSP uses the primary key `cusip`. These keys do not have a one-to-one
290 mapping because it is possible for assets to be delisted, to be added to the dataset during a calendar
291 month, or to change primary keys (for example, due to company mergers or acquisitions). Because
292 we batch data by month and year, we can construct a one-to-one mapping between `secid` and
293 `cusip` using the WRDS link tables (`wrdsapps_link_crsp_optionm` and the `stocknames__v2`
294 table, which provide the start and end dates during which each primary key is active. For each month
295 of data we drop any rows where the `cusip` or `secid` is valid for only part of the month.

296 **A.2 Data Collection**

297 Using our table of valid primary keys, we downloaded raw data from OptionMetrics IvyDB, using
298 the Volatility Surfaces and Realized Volatility tables, and the end-of-day return from the CRSP Stock
299 dataset. The IV surface dataset contains smoothed, interpolated data on standardized calls and puts,
300 with expirations of 10,30, 60, 91, 122, 152, 182, 273, 365, 547, and 730 calendar days, at deltas
301 of 0.10, 0.15, 0.20, 0.25, 0.30, 0.35, 0.40, 0.45, 0.50, 0.55, 0.60, 0.65, 0.70, 0.75, 0.80, 0.85, 0.90
302 (negative deltas for puts). We fuse this data on the primary key and date, producing a total of 120
303 parquet files (12 months each from 2012 to 2022).

304 Rows are dropped if there is missing data in the IV surface or invalid values in the CRSP stock price
305 or return values, indicating assets that did not trade on a particular day. We construct the IV surface
306 using all available δ values and days-to-expiry for both calls and puts. We do not attempt to filter for
307 outliers in the IV surfaces or other data.

308 Our final dataset consists of 4,259,070 rows, distributed across months as shown in Figure 5.

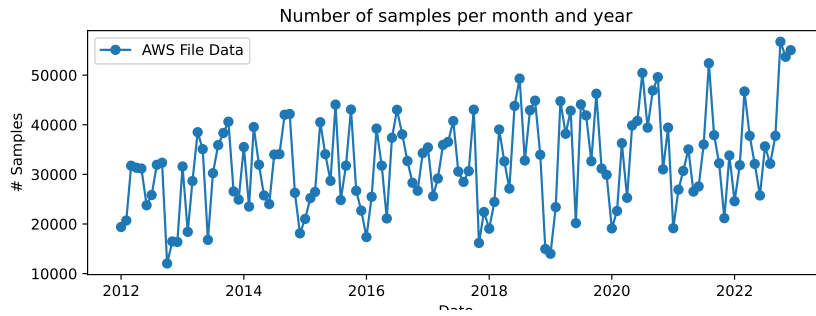


Figure 5: Number of samples per month of data.

309 **B Model Definitions**

310 Table 4 lists the parameters used to initialize the various model architectures.

311 The Vision Transformer architecture is taken from the standard PyTorch implementation³, modified
 312 to accept tensors of size $\mathbb{R}^{1 \times 10 \times 36}$ instead of square RGB images.

313 All models considered take input of size 10×36 , operate on 2×2 image patches, following the
 314 approach in Kelly et al. [2023], and produce a single real-valued prediction. Models consist of a
 315 Vision Transformer (ViT) followed by a 4-layer multilayer perceptron (MLP) to convert the ViT
 316 vector output into a single prediction.

Model	# ViT Layers	# Heads	# ViT hidden dim.	ViT MLP dim.	ViT Dropout	ViT output size	MLP hidden dim.
ViT_0.005M_wide	1	8	64	64	0.1	64	64
ViT_0.12M_deep	4	8	64	64	0.1	64	64
ViT_0.17M_wide	1	16	128	128	0.1	128	128
ViT_0.5M_deep	4	16	128	128	0.1	128	128
ViT_0.5M_wide	1	16	256	256	0.1	256	128
ViT_1.7M	4	16	256	256	0.1	256	128

Table 4: Summary of model parameters for all model sizes.

317 To conduct the MLP-only ablation experiment, we define the following alternate models, selected to
 318 match the parameter sizes of the ViT models.

- 319 • MLP_0_12: A four-layer MLP with input size = 360 (to match the flattened IV surface) and
 320 hidden size = 180.
- 321 • MLP_0_17: A four-layer MLP with input size = 360 and hidden size = 240.
- 322 • MLP_0_5: An eight-layer MLP with input size = 360 and hidden size = 350.

323 **B.1 torchinfo summary of MLP_0_5 model**

324 This summary was generated with an input and hidden size of 360, matching the size used in the
 325 ablation test.

```

326 =====
327 Layer (type:depth-idx)                Output Shape                Param #
328 =====
329 DeepMLP                                [1, 1]                      --
330 Linear: 1-1                            [1, 360]                    129,960
331 BatchNorm1d: 1-2                       [1, 360]                    720
332 ReLU: 1-3                              [1, 360]                    --
333 Linear: 1-4                            [1, 360]                    129,960
334 BatchNorm1d: 1-5                       [1, 360]                    720
335 ReLU: 1-6                              [1, 360]                    --
336 Linear: 1-7                            [1, 360]                    129,960
337 BatchNorm1d: 1-8                       [1, 360]                    720
338 ReLU: 1-9                              [1, 360]                    --
339 Linear: 1-10                           [1, 180]                    64,980
340 BatchNorm1d: 1-11                      [1, 180]                    360
341 ReLU: 1-12                             [1, 180]                    --
342 Linear: 1-13                           [1, 180]                    32,580
343 BatchNorm1d: 1-14                      [1, 180]                    360
344 ReLU: 1-15                             [1, 180]                    --
345 Linear: 1-16                           [1, 90]                     16,290
346 BatchNorm1d: 1-17                     [1, 90]                     180
  
```

³https://docs.pytorch.org/vision/main/models/vision_transformer.html

```

347 ReLU: 1-18                [1, 90]                --
348 Linear: 1-19              [1, 90]                8,190
349 BatchNorm1d: 1-20         [1, 90]                180
350 ReLU: 1-21                [1, 90]                --
351 Linear: 1-22               [1, 1]                 91
352 =====
353 Total params: 515,251
354 Trainable params: 515,251
355 Non-trainable params: 0
356 Total mult-adds (Units.MEGABYTES): 0.52
357 =====

```

358 B.2 torchinfo summary of all other MLP models

359 This summary was generated with an input size of 256 and a hidden size of 128.

```

360 =====
361 Layer (type:depth-idx)      Output Shape            Param #
362 =====
363 SimpleMLP                  [1, 1]                 --
364 Linear: 1-1                 [1, 128]               32,896
365 BatchNorm1d: 1-2           [1, 128]               256
366 ReLU: 1-3                  [1, 128]               --
367 Linear: 1-4                 [1, 128]               16,512
368 BatchNorm1d: 1-5           [1, 128]               256
369 ReLU: 1-6                  [1, 128]               --
370 Linear: 1-7                 [1, 64]                8,256
371 BatchNorm1d: 1-8           [1, 64]                128
372 ReLU: 1-9                  [1, 64]                --
373 Linear: 1-10                [1, 1]                 65
374 =====
375 Total params: 58,369
376 Trainable params: 58,369
377 Non-trainable params: 0
378 Total mult-adds (Units.MEGABYTES): 0.06
379 =====

```

380 C Additional Results

381 Figure 6 shows the training trajectories for small and large ViT models, showing how many models
382 achieve their full performance on one or two epochs.

383 We observe that while training on one year of data can produce good results, they are often inconsistent.
384 Further, we observe the expected relationship between the number of model parameters and the data
385 required to train the model; the smallest models perform best on small datasets, and the largest model
386 requires the full dataset: 10 years of training data, with 1 year of test data.

387 Figure 7 shows the Huber loss, recorded at each batch, for some samples of 1, 4, and 10-year training
388 runs. We observe a few loss spikes, which may be caused when the cosine learning rate increases,
389 although in most cases the learning rate increase does not cause a spike.

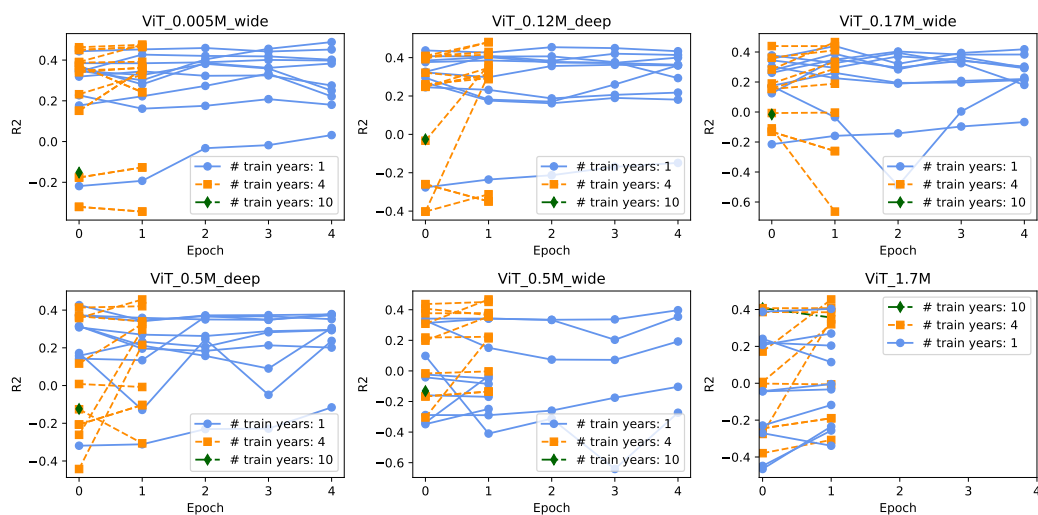


Figure 6: R^2 plotted over the number of training epochs, broken down by ViT model type. All of the train-on-one-year, test-on-one-year models exhibit poor performance when tested on 2020 data, corresponding to a single low or negative R^2 trajectory observed in each plot.

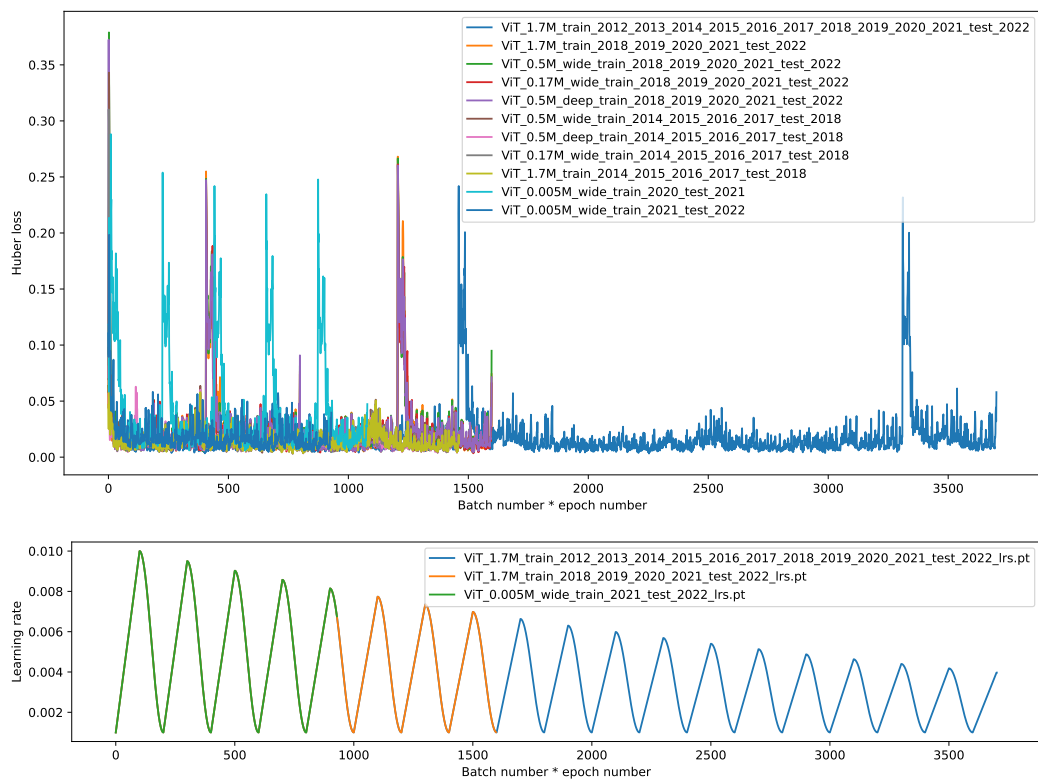


Figure 7: Huber loss and cosine learning rate for several sampled training runs.